

3D SOURCE LOCALIZATION IN THE SPHERICAL HARMONIC DOMAIN USING A PSEUDOINTENSITY VECTOR

Daniel P. Jarrett, Emanuël A.P. Habets and Patrick A. Naylor

Dept. of Electrical & Electronic Engineering, Imperial College London
Exhibition Road, SW7 2BT, London, UK
email: {daniel.jarrett05, e.habets, p.naylor} @imperial.ac.uk

ABSTRACT

The problem of acoustic source localization is important in many acoustic signal processing applications, such as distant speech acquisition and automated camera steering. In noisy and reverberant environments, the source localization problem becomes challenging and many existing algorithms deteriorate. Three-dimensional source localization presents advantages for certain applications such as beamforming, where we can steer a beam to both the desired azimuth and the desired elevation. In this paper, we present an acoustic source localization method with low computational complexity which, instead of using individual microphone signals, combines them to form eigenbeams. We then use the zero- and first-order eigenbeams to compute a pseudointensity vector pointing in the direction of the sound source. In an experimental study, the proposed method's localization accuracy is compared with that of a steered response power localization method, which uses the same eigenbeams. The results demonstrate that the proposed method has higher localization accuracy.

1. INTRODUCTION

While linear and planar microphone arrays have been the subject of much research, and are now relatively well understood, spherical microphone arrays, on the other hand, have only recently become a topic of interest. They offer the advantage of being able to analyze sound fields in three dimensions, and in this paper we will look at their ability to perform source localization in three dimensions, which is useful in applications such as beamforming for hands-free telephony, noise source identification (in vehicles or aircraft), or automatic camera steering.

Acoustic localization in two dimensions has been widely studied, using time difference of arrival (TDOA) based methods, subspace-based methods (ESPRIT, MUSIC), or steered response power (SRP). MUSIC [1] and ESPRIT [2] have also been generalized to three dimensions, although they are computationally inefficient due to the need for an exhaustive search, and are typically not robust to reverberation.

In this paper, we propose a new method of three-dimensional source localization for a single active source, based on a pseudointensity vector, pointing in the direction of the sound source. This vector is calculated using eigenbeams which describe the sound pressure signals in the spherical harmonic domain. We compare this method to a spherical

harmonic domain implementation of the SRP method which is commonly used in the time and frequency domains.

This paper is organized as follows: in Section 2 we introduce background theory relevant to spherical harmonics, in Section 3 we introduce the SRP method, in Section 4 we present the pseudointensity vector, in Section 5 we briefly discuss the computational complexity of the two methods and finally in Section 6 we evaluate their accuracy.

2. SPHERICAL HARMONICS

In this section, we briefly review some of the theory behind spherical harmonics. For a more exhaustive introduction, the reader is referred to [3, 4, 5].

Consider a sound pressure field at a point $(r, \Omega) \triangleq (r, \theta, \phi)$ (in spherical polar coordinates, with elevation θ and azimuth ϕ), denoted by $p(k, r, \Omega)$, where k is the wavenumber. The raw acquired pressure signals $p(n, r, \Omega)$ are in the discrete-time domain, and hence first need to be Fourier-transformed to give $p(k, r, \Omega)$. The spherical Fourier transform of this field is then given by [3, p. 192]:

$$p_{lm}(k, r) = \int_{\Omega \in S^2} p(k, r, \Omega) Y_{lm}^*(\Omega) d\Omega, \quad (1)$$

where $\int_{\Omega \in S^2} d\Omega \triangleq \int_0^{2\pi} \int_0^\pi \sin \theta d\theta d\phi$, and $(\cdot)^*$ denotes the complex conjugate.

The spherical harmonics $Y_{lm}(\Omega)$ of order l and degree m , are given by [3, p. 190]:

$$Y_{lm}(\Omega) = \sqrt{\frac{(2l+1)(l-m)!}{4\pi(l+m)!}} P_{lm}(\cos \theta) e^{im\phi}, \quad (2)$$

where P_{lm} is the associated Legendre function and $i = \sqrt{-1}$. They exhibit an orthogonality property which we will make use of when calculating the sound field in the spherical harmonic domain [3, p. 191]:

$$\int_{\Omega \in S^2} Y_{lm}(\Omega) Y_{pq}^*(\Omega) d\Omega = \delta_{lp} \delta_{mq}, \quad (3)$$

where δ is defined as follows:

$$\delta_{ij} = \begin{cases} 1, & \text{if } i = j; \\ 0, & \text{if } i \neq j. \end{cases} \quad (4)$$

The pressure field can be calculated from the Fourier transform using the inverse relation:

$$p(k, r, \Omega) = \sum_{l=0}^{\infty} \sum_{m=-l}^l p_{lm}(k, r) Y_{lm}(\Omega). \quad (5)$$

The authors acknowledge the financial support of the Future and Emerging Technologies (FET) programme within the Seventh Framework Programme for Research of the European Commission, under FET-Open grant number: 226007 SCENIC

If we assume that a sound source is in the far-field, the wavefront impinging on a spherical array of radius r_a can be assumed to be planar, and if we call its arrival direction Ω_0 , we can write p_{lm} as [6]:

$$p_{lm}(k, r) = a(k)b_l(kr, kr_a)Y_{lm}^*(\Omega_0), \quad (6)$$

where $a(k)$ is the wave amplitude and $b_l(kr, kr_a)$ are the *mode coefficients* or *mode strengths*. For the sound field on the surface of a rigid sphere (as used in our experimental study), again assuming far-field conditions [3, p. 228]:

$$b_l(kr, kr_a) = 4\pi i^l \left[\mathcal{J}_l(kr) - \frac{\mathcal{J}'_l(kr_a)}{\mathcal{H}_l^{(2)'}(kr_a)} \mathcal{H}_l^{(2)}(kr) \right], \quad (7)$$

where \mathcal{J}_l is the spherical Bessel function of order l , $\mathcal{H}_l^{(2)}$ is the spherical Hankel function of the second kind and of order l , and $(\cdot)'$ denotes the first derivative with respect to kr . As our microphones are on the surface of the sphere, we let $r = r_a$ and define $b_l(k) \triangleq b_l(kr_a, kr_a)$.

In a system with M microphones whose polar coordinates are (r_q, Ω_q) , $q = 1, \dots, M$, we must approximate the integral in (1) with a sum:

$$p_{lm}(k) \approx \sum_{q=1}^M g_{q,lm} p(k, r_q, \Omega_q). \quad (8)$$

Weights $g_{q,lm}$ are chosen to ensure that (8) is an accurate approximation of (1). The number of microphones M must be sufficiently high: if N is the highest harmonic order, $p(k, r, \Omega)$ has $(N+1)^2$ independent harmonics ($\sum_{l=0}^N \sum_{m=-l}^l 1 = \sum_{l=0}^N (2l+1) = (N+1)^2$), therefore in order to not lose information, we need to sample with at least this many microphones. The number of microphones M must therefore satisfy [5]:

$$M \geq (N+1)^2. \quad (9)$$

3. LOCALIZATION USING THE STEERED RESPONSE POWER

As a baseline for comparison, we will now present a conventional method for source localization: computing a map of the SRP which allows us to find the direction with the highest power. In order to produce this acoustic map, we must first introduce the theory of beamforming in the spherical harmonic domain.

3.1 Beamforming

The spherical Fourier transform allows us to represent the sound field in terms of orthogonal basis functions and can therefore be interpreted as an eigenbeamformer. The signals $p_{lm}(k)$ that result from the spherical Fourier transform are known as eigenbeams [4] and can be interpreted as individual sensors in the classical sensor array processing framework. It is important to note that the directivity pattern of the eigenbeams is frequency invariant while each magnitude response depends on the order l . Once we have computed the eigenbeams, we can synthesize an arbitrary beam pattern by applying a modal beamformer. In general, the output of the modal beamformer can be expressed by

$$y(k) = \sum_{l=0}^N \sum_{m=-l}^l w_{lm}^*(k) p_{lm}(k), \quad (10)$$

where N is the highest array order and $w_{lm}(k)$ are the beamforming weights in the spherical harmonic domain. Often it is sufficient to use a beam pattern which is rotationally symmetric around the look direction Ω_u [7]:

$$w_{lm}^*(k, \Omega_u) = \frac{d_l(k)}{b_l(k)} Y_{lm}(\Omega_u), \quad (11)$$

where $d_l(k)$ allows us to change the beam pattern. While the above interpretation has some practical advantages, it should be noted that the inverse spherical Fourier transform given by (5) is done implicitly as it is incorporated into the beamformer weights.

By combining (10) and (11) and reorganizing the terms we obtain

$$y(k, \Omega_u) = \sum_{l=0}^N \sum_{m=-l}^l \frac{d_l(k)}{b_l(k)} p_{lm}(k) Y_{lm}(\Omega_u) \quad (12a)$$

$$= \sum_{l=0}^N \frac{d_l(k)}{b_l(k)} \sum_{m=-l}^l Y_{lm}(\Omega_u) p_{lm}(k). \quad (12b)$$

As shown in (12b) we can compute the output of the beamformer in two steps. In the first step (second term on the right hand side) the beamformer is steered to the look direction Ω_u . In the second step (first term on the right hand side) the beam pattern is synthesized.

3.2 Steered Response Power Map

An acoustic map can be computed and depicted in different ways. Here we choose to compute the power corresponding to the output of a beamformer steered in different directions. The location with the highest power provides an estimate of the location of the sound source. It should be noted that the power of the beamformer output does not relate to one particular spatial location. The resolution of the acoustic map depends on the directivity pattern of the beamformer (which in turn depends on the highest array order N), and the number of beams for which power is measured.

We take advantage of the orthogonality of the spherical harmonics in (3) and choose weights $g_{q,lm}$ given by:

$$g_{q,lm} = \frac{4\pi}{M} Y_{lm}^*(\Omega_q), \quad (13)$$

which makes the approximation in (8) exact if (9) is satisfied and our microphones are equally spaced on the sphere. However for non-trivial microphone configurations, it is not possible for the microphones to be perfectly equidistant, therefore there is a small error involved.

By substituting the expression for the weights $g_{q,lm}$ in (13) into (8) we obtain:

$$p_{lm}(k) \approx \frac{4\pi}{M} \sum_{q=1}^M Y_{lm}^*(\Omega_q) p(k, r_q, \Omega_q), \quad (14)$$

and substituting this expression into the beamformer output $y(k)$ expression in (12b), if we choose $d_l(k) = 1$ (which maximizes the directivity [8]), we find:

$$y(k, \Omega_u) \approx \frac{4\pi}{M} \sum_{l=0}^N \frac{1}{b_l(k)} \sum_{m=-l}^l Y_{lm}(\Omega_u) \sum_{q=1}^M Y_{lm}^*(\Omega_q) \cdot p(k, r_q, \Omega_q). \quad (15)$$

The spherical harmonics Y_{lm} for angles Ω_u (the angles of our beams) can be efficiently computed from those for angles Ω_q (the angles of our microphones) using the addition-theorem for Legendre functions.

Once we have the beamformer output as a function of the look direction Ω_u , we can compute a power map $\mathcal{M}(\Omega_u)$ at a certain number of points on a sphere with polar coordinates $\Omega_u \triangleq (\theta_u, \phi_u)$:

$$\mathcal{M}(\Omega_u) = \sum_k \beta(k) |y(k, \Omega_u)|^2, \quad (16)$$

where $\beta(k)$ is a weighting function which allows us to, for example, ignore all beams based on recordings below a certain frequency, which are likely to contain low frequency noise and little speech, or to apply an A-weighting function. We can also smooth the map over multiple time frames. In our experimental study, we applied a moving average filter.

Assuming a single active source, the source location Ω_s is then the direction with maximum power:

$$\Omega_s = \arg \max_{\Omega_u} \mathcal{M}(\Omega_u). \quad (17)$$

4. LOCALIZATION USING THE PSEUDOINTENSITY VECTOR

4.1 Motivation

Unfortunately the SRP method, while intuitively simple, is computationally complex: as the cost function $\mathcal{M}(\Omega_u)$ is non-convex, we must steer a beam in every direction to determine which direction has the highest power, and hence where the sound source is likely to be located. We now present a novel alternative method based on intensity vectors.

In acoustics, sound intensity is a measure of the flow of sound energy through a surface per unit area, in a direction perpendicular to this surface. The idea of a pseudointensity vector is inspired by the concept of intensity vectors, defined as [9]:

$$\mathbf{I} = \frac{1}{2} \text{Re} \{ p^* \cdot \mathbf{v} \}, \quad (18)$$

where p is the sound pressure, $\mathbf{v} = [v_x v_y v_z]^T$ is the particle velocity vector, v_a (with $a \in \{x, y, z\}$) is the particle velocity in the i^{th} direction (with a dipole directivity pattern), and $\text{Re}\{\cdot\}$ denotes the real part of a complex number. For a plane wave,

$$\mathbf{v} = -\frac{p}{\rho_0 c} \mathbf{u} \quad (19)$$

where c is the speed of sound in the medium, ρ_0 is the ambient density, and \mathbf{u} is a unit vector pointing towards the acoustic source.

The intensity vector corresponds to the magnitude and direction of the transport of acoustical energy, indicating its utility for determining the direction of arrival (DOA) of a sound wave. Unfortunately in practice it is difficult to measure particle velocity, although attempts have been made using vibrating surfaces and accelerometers, or more successfully, using the finite difference method with two-microphone arrays [9]. More recently particle velocity has been measured with a micromachined transducer, the Microflow [10]. In order to be able to use only one type of sensor, we would like to compute the intensity vector using a spherical microphone array.

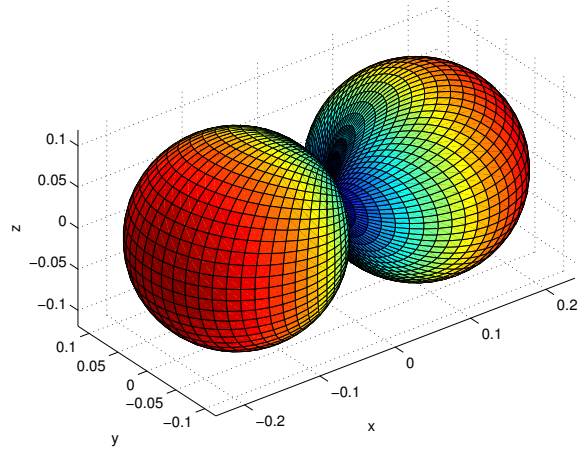


Figure 1: Beam pattern of a linear combination of spherical harmonics, aligned to the x-axis: $|\alpha_{x,(-1)} Y_{1(-1)}(\theta, \phi) + \alpha_{x,0} Y_{10}(\theta, \phi) + \alpha_{x,1} Y_{11}(\theta, \phi)|$.

4.2 Definition

We propose a pseudointensity vector $\mathbf{I}(k)$ which is conceptually similar to an intensity vector, but is calculated using the zero- and first-order eigenbeams $p_{lm}(k)$ ($l = 0, 1$), and is defined as follows:

$$\mathbf{I}(k) = \frac{1}{2} \text{Re} \left\{ \left(\frac{p_{00}(k)}{b_0(k)} \right)^* \begin{bmatrix} p_x(k) \\ p_y(k) \\ p_z(k) \end{bmatrix} \right\} \quad (20)$$

where the first term, $(p_{00}(k)/b_0(k))^*$ is the complex conjugate of the omnidirectional sound pressure signal, and the second term corresponds to the particle velocity vector in (18). The components $p_x(k)$, $p_y(k)$ and $p_z(k)$ of this vector are dipoles steered in the opposite direction to the x, y and z axes which are proportional to the particle velocity. Since we are only interested in the pseudointensity vector's direction, the scale factor $(\rho_0 c)^{-1}$ is omitted here.

In order to form the beams $p_x(k)$, $p_y(k)$ and $p_z(k)$, we make use of the available eigenbeams $p_{1(-1)}(k)$, $p_{10}(k)$ and $p_{11}(k)$. This can be done by forming a linear combination of rotated eigenbeams:

$$p_a(k) = \frac{1}{b_1(k)} \sum_{m=-1}^1 \alpha_{a,m} p_{1m}(k), \quad a \in \{x, y, z\} \quad (21)$$

where the $b_1(k)$ factor is required to make the beam patterns wavenumber independent.

To rotate each of the eigenbeams in the appropriate direction (θ_r, ϕ_r) , we multiply them by the spherical harmonics $Y_{1m}(\theta_r, \phi_r)$. It can be shown that we therefore require:

$$\alpha_{x,m} = Y_{1m}(\pi/2, \pi), \quad (22a)$$

$$\alpha_{y,m} = Y_{1m}(\pi/2, -\pi/2), \quad (22b)$$

$$\alpha_{z,m} = Y_{1m}(\pi, 0). \quad (22c)$$

The beam pattern of p_x , which is aligned to the x-axis, is shown as an example in Fig. 1.

4.3 Localization

The pseudointensity vector is calculated for every discrete wavenumber; we therefore have a number of vectors which

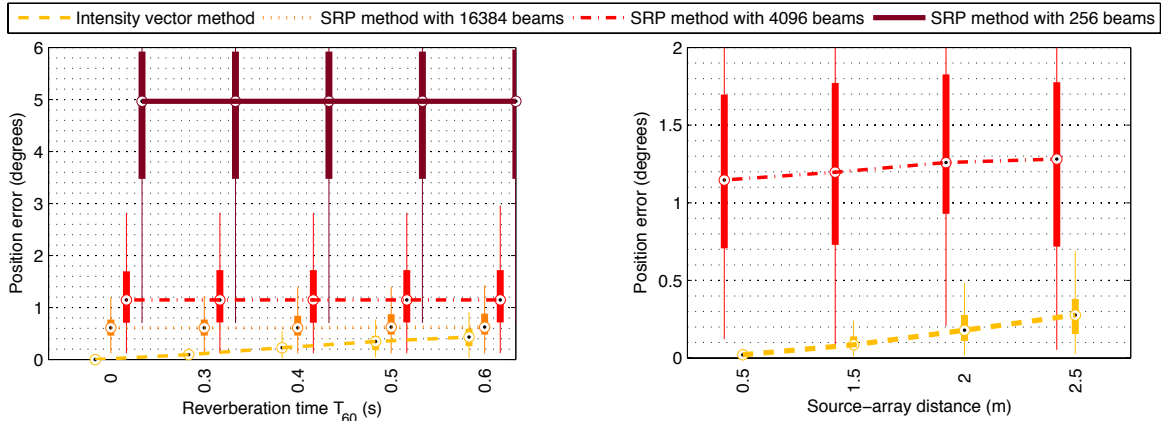


Figure 2: Position errors for the SRP and pseudointensity vector methods as a function of reverberation time (left) and source-array distance (right). In the first case (left) the source-array distance is 1.5 m and ensures that the direct to reverberation energy ratio remains above 0 dB. In the second case (right) the reverberation time is 300 ms. The boxes show the median, upper and lower quartiles, and the whiskers extend to 1.5 times the interquartile range.

point in slightly different directions. While they provide an approximate location for the sound source, some averaging is necessary to locate it more precisely. The intensity vector averaged across frequency is given by:

$$\mathbf{I} = \sum_k \gamma(k) \mathbf{I}(k) \quad (23)$$

where $\gamma(k)$ is a weighting function similar to $\beta(k)$ in (16). Note that even with $\gamma(k) = 1, \forall k$ we are implicitly giving a higher weight to the intensity vectors with the highest norm.

An estimate of the unit vector \mathbf{u} pointing in the direction of the sound source, as in (19), is given by:

$$\hat{\mathbf{u}} = \frac{\mathbf{I}}{\|\mathbf{I}\|} \quad (24)$$

where $\|\cdot\|$ indicates a vector's ℓ_2 norm. When multiple time frames are available, one can additionally smooth $\hat{\mathbf{u}}$ over time.

5. COMPUTATIONAL COMPLEXITY

The pseudointensity method requires only the computation of the four zero- and first-order eigenbeams, and three weighted averages $p_x(k)$, $p_y(k)$ and $p_z(k)$ of these eigenbeams. The SRP method, on the other hand, requires us to compute these eigenbeams, and additionally steer beams in all directions as shown in (12).

A fair comparison of these two methods would therefore be to compute the SRP with only three beams, however for this number of beams it is impossible to obtain a reasonable DOA estimate from SRP. As we will see in Section 6, to obtain accuracy of the same order as the pseudointensity vector method, we must steer several thousands of beams.

In practice, however, it is not efficient to steer this many beams indiscriminately in all directions: a coarse grid approach can be taken at first, to determine the DOA within $\pm 30^\circ$, for example, and we can then apply a finer grid to the area of interest, thus reducing the amount of unnecessary detail in areas where the acoustic source cannot be located (based on the results of the first search).

6. PERFORMANCE EVALUATION

6.1 Using simulated data

In order to evaluate objectively the accuracy of the pseudointensity vector as a localization method, we must be able to generate pseudointensity vectors in a simulated environment where the true source positions are known precisely. We achieve this by using a Room Impulse Response Generator [11] based on Allen & Berkley's image method [12], which allows us to generate the three necessary beams $p_x(k)$, $p_y(k)$ and $p_z(k)$. Using these beams and (21), we can also recover the first order eigenbeams $p_{1(-1)}(k)$, $p_{10}(k)$ and $p_{11}(k)$ in order to compute the SRP.

In order to evaluate and compare the performance of these two localization methods, we choose to calculate the angle ε between a vector pointing in the correct direction \mathbf{u} , and a vector pointing in the direction estimated by either of the two methods $\hat{\mathbf{u}}$, as in [13]. If these vectors are normalized, ε is given by:

$$\varepsilon = \cos^{-1}(\mathbf{u}^T \hat{\mathbf{u}}) \quad (25)$$

For these simulations we place a receiver close to the center of a room with dimensions $10 \times 8 \times 12$ m in which a single source is present. The source signal consists of a white Gaussian noise sequence of duration 1 s. We choose a sampling frequency of 8 kHz and a frame length of 32 ms with a 50% overlap. We use the same number of eigenbeams for the SRP as for the pseudointensity vector, i.e. we choose the limit $N = 1$. We do not apply any weighting in (16) and (23), that is, we set $\beta(k) = \gamma(k) = 1, \forall k$.

In the first simulation, the reverberation time T_{60} is varied from 0 (anechoic room) to 600 ms while the source-array distance is fixed at 1.5 m. With such a configuration, reverberation times between 300 and 600 ms correspond to direct to reverberant energy ratios between approximately 10 and 0 dB. In the second simulation the source-array distance ranges between 0.5 and 2.5 m while the reverberation time is fixed at 300 ms.

A statistical analysis of the results of these simulations is shown in Fig. 2 (the boxes show the median, upper and lower quartiles, and the whiskers extend to 1.5 times the interquartile range), based on Monte Carlo simulations with

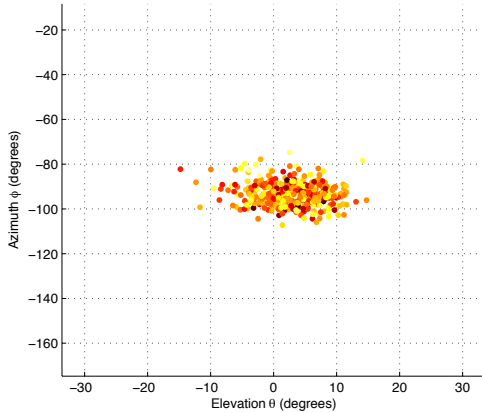


Figure 3: Plot of pseudointensity vector elevations and azimuths for a source at approximately $(0^\circ, -90^\circ)$. The darkness of the data points indicates the norm of the corresponding vector.

100 runs. For each run a new DOA was randomly selected from a uniform distribution around the sphere. The accuracy of the pseudointensity vector method is significantly higher than that of the SRP method with a small number of beams (4096 or less). For a larger number of beams (16384), the pseudointensity vector method still outperforms the SRP method, but by a smaller margin. This is still the case even as the source-array distance increases above 2 m.

6.2 Using spherical microphone array measurements

To experimentally test our proposed method, we measure a sound field using an em32 Eigenmike from mh acoustics, which is a spherical microphone array of radius $r_a = 4.2$ cm with $M = 32$ microphones. We choose $N = 1$. Measurements are taken in a room with dimensions $2.9 \times 2.7 \times 3.3$ m with a reverberation time of approximately 300 ms.

Unfortunately as it was not possible to take precise measurements of the true DOAs, a quantitative assessment of the accuracy of the two methods would not be meaningful, however for illustrative purposes Fig. 4 shows a power map obtained using the SRP method, and Fig. 3 is a plot of the azimuths and elevations of some pseudointensity vectors we obtained for a source located at approximately $(0^\circ, -90^\circ)$. In Fig. 3 we note a cluster of DOA estimates centered around the correct DOA, and Fig. 4 confirms that the direction of highest power corresponds to this same DOA.

7. CONCLUSION

The pseudointensity vector offers the possibility of fast source localization without the computational complexity of steering beams in all directions. Furthermore the results it yields are relatively accurate when compared to the SRP method with a viable number of beams: in typical environments the mean error is below 0.5° .

REFERENCES

[1] D. Khaykin and B. Rafaely, "Coherent signals direction-of-arrival estimation using a spherical microphone array: Frequency smoothing approach," in *Proc. IEEE Workshop on Applications of Signal Processing to Audio and Acoustics*, Oct. 2009, pp. 221–224.

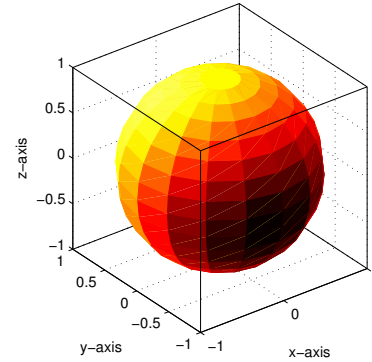


Figure 4: Power map for a source at approximately $(0^\circ, -90^\circ)$, with 256 beams. The darkest areas correspond to the beams with highest power.

[2] H. Teutsch and W. Kellermann, "Eigen-beam processing for direction-of-arrival estimation using spherical apertures," in *Proc. Joint Workshop on Hands-Free Speech Communication and Microphone Arrays*. Piscataway, New Jersey, USA: IEEE, Mar. 2005.

[3] E. G. Williams, *Fourier Acoustics: Sound Radiation and Nearfield Acoustical Holography*, 1st ed. Academic Press, 1999.

[4] J. Meyer and T. Agnello, "Spherical microphone array for spatial sound recording," in *Proc. Audio Eng. Soc. Conventions*, New York, NY, USA, Oct. 2003, pp. 1–9.

[5] B. Rafaely, "Analysis and design of spherical microphone arrays," *IEEE Trans. Speech Audio Process.*, vol. 13, no. 1, pp. 135–143, Jan. 2005.

[6] —, "Plane-wave decomposition of the pressure on a sphere by spherical convolution," *J. Acoust. Soc. Am.*, vol. 116, no. 4, pp. 2149–2157, Oct. 2004.

[7] J. Meyer and G. Elko, "A highly scalable spherical microphone array based on an orthonormal decomposition of the soundfield," in *Proc. IEEE Intl. Conf. on Acoustics, Speech and Signal Processing (ICASSP)*, vol. 2, May 2002, pp. 1781–1784.

[8] B. Rafaely, Y. Peled, M. Agmon, D. Khaykin, and E. Fisher, "Spherical microphone array beamforming," in *Speech Processing in Modern Communication: Challenges and Perspectives*, I. Cohen, J. Benesty, and S. Gannot, Eds. Springer, Jan. 2010, ch. 11.

[9] M. J. Crocker and F. Jacobsen, "Sound intensity," in *Handbook of Acoustics*, M. J. Crocker, Ed. Wiley-Interscience, 1998, ch. 106, pp. 1327–1340.

[10] H.-E. de Bree, P. Leussink, T. Korthorst, H. Jansen, T. S. Lammerink, and M. Elwenspoek, "The μ -flown: a novel device for measuring acoustic flows," vol. 54, no. 1-3. Elsevier, 1996, pp. 552–557.

[11] E. A. P. Habets. (2008, May) Room impulse response (RIR) generator. [Online]. Available: <http://home.tiscali.nl/ehabets/rirgenerator.html>

[12] J. B. Allen and D. A. Berkley, "Image method for efficiently simulating small-room acoustics," *J. Acoust. Soc. Am.*, vol. 65, no. 4, pp. 943–950, Apr. 1979.

[13] J. Bermudez, R. C. Chin, P. Davoodian, A. T. Y. Lok, Z. Aliyazicioglu, and H. K. Hwang, "Simulation study on DOA estimation using ESPRIT algorithm," in *Proc. World Congress on Engineering and Computer Science (WCECS)*, vol. 1, 2009, pp. 431–436.